Epitaxial Nature of the Films of $LaNiO_3$, $Pb(Zr_{0.5}Ti_{0.5})O_3$, and $La_{0.95}Mn_{0.95}O_3$ Obtained by Nebulized Spray Pyrolysis

Hemantkumar N. Aiyer, A. R. Raju, G. N. Subbanna, and C. N. R. Rao*

Materials Research Centre and CSIR Centre of Excellence in Chemistry, Indian Institute of Science, Bangalore 560012, India, and Jawaharlal Nehru Centre for Advanced Scientific Research, Jakkur, Bangalore 560064, India

Received September 4, 1996. Revised Manuscript Received December 19, 1996[⊗]

Films of complex oxide materials deposited on single-crystal substrates by means of nebulized spray pyrolysis have been investigated for their epitaxial nature by employing X-ray rocking curve studies and high-resolution electron microscopy, the latter enabling a direct study of the interface between the film and the substrate. It has been demonstrated that films of metallic $LaNiO_3$, ferroelectric $Pb(Zr_{0.5}Ti_{0.5})O_3$, and $La_{0.95}Mn_{0.95}O_3$ exhibiting giant magnetoresistance, deposited by nebulized spray pyrolysis on $SrTiO_3(100)$ or $LaAlO_3(100)$ are all epitaxial. Nebulized spray pyrolysis is a valuable inexpensive tool to deposit epitaxial films of complex oxide materials.

1. Introduction

Epitaxial films of oxide materials are generally prepared by a variety of deposition techniques which include pulsed laser deposition (PLD), metal−organic chemical vapor deposition (MOCVD), and molecular beam epitaxy (MBE).[1] For example, epitaxial films of ferroelectric $PbZr_xTi_{1-x}O_3$ and $PbTiO_3$ have been obtained by MOCVD[2−5] as well as PLD.[6,7] Epitaxial films of manganates of the composition $La_{1-x}A_xMnO_{3+\delta}$ (A = Ca, Sr, Ba) showing giant magnetoresistance have been deposited recently by PLD.[8,9] Epitaxial films of metallic $LaNiO_3$ have been prepared by PLD.[10]

Recently, we reported that thin films of complex oxide materials can be deposited on suitable single-crystal substrates by means of nebulized spray pyrolysis which is a simple, chemical method.[11] Nebulized spray pyrolysis involves the atomization of a solution containing organometallic precursors in a suitable solvent, followed by the pyrolysis of the atomized spray resulting in the deposition of an oxide film on the solid substrate. Although this method was shown to be effective in obtaining oriented films of oxide materials by means of X-ray diffraction ($\theta-\theta$ scan), it was not clear whether these films were epitaxial. In view of the increasing importance of epitaxial films of oxide materials in a variety of technological applications, we have carried out an investigation of thin films of oxides such as $LaNiO_3$ (LNO), $PbZr_xTi_{1-x}O_3$ (PZT), and $LaMnO_3$ (LMO) deposited on single-crystal substrates by nebulized spray pyrolysis for their epitaxial nature, the LMO films having been deposited by this technique for the first time. We have employed scanning electron microscopy (SEM), X-ray diffraction (θ and ω rocking curve scans) and high-resolution transmission electron microscopy (HRTEM) for the study of these films. Of particular importance in the study is the examination of the interface between the substrate and the film by high-resolution TEM.

2. Experimental Section

The films were deposited using a home-built ultrasonically nebulized spray pyrolysis system.[11] A solution containing the organometallic derivatives of the relevant metals in a suitable solvent is nebulized by making use of a PZT transducer. The nebulized spray is slowly deposited on a solid substrate at a relatively low temperature with a sufficient control of the rate of deposition to yield the oxide film of the desired stoichiometry. The film thickness can vary from a few hundred nanometers to a few microns, depending on the solution concentration, deposition time, etc.

Films of the various oxide materials were deposited by nebulizing the appropriate stoichiometric mixture of organometallic precursors in methanol solvent (0.1 M). To deposit the films of $LaNiO_3$, acetylacetonates of lanthanum and nickel were used as precursors. $LaNiO_3$ films were deposited on $SrTiO_3(100)$ substrates at 675 K for 8 h and air annealed at the same temperature for 12 h. PZT films were deposited by employing lead acetate, zirconium isopropoxide, and titanium isopropoxide as precursors. These films were deposited on $SrTiO_3(100)$ substrates at 625 K for 3 h and then air annealed for 12 h at the same temperature. For depositing $LaMnO_3$

* To whom correspondence should be addressed at the Indian Institute of Science.

[⊗] Abstract published in *Advance ACS Abstracts,* February 1, 1997.

(1) Fork, D. K.; Phillips, J. M.; Ramesh, R.; Wolf, R. M. *Epitaxial Oxide Thin Films and Heterostructures*; Materials Research Society: Pittsburgh, 1994; p 341.
(2) Sakashita, Y.; Ono, T.; Segawa, H.; Tominaga, K.; Okada, M. *J. Appl. Phys.* **1991**, *69*, 8352.
(3) Foster, C. M.; Li, Z.; Bai, G. R.; You, H.; Guo, D.; Chang, H. L. M *Mater. Res. Soc. Symp. Proc.* **1994**, *341*, 295.
(4) Bai, G. R.; Chang, H. L. M.; Foster, C. M.; Shen, Z.; Lam, D. J. *J. Mater. Res.* **1994**, *9*, 156.
(5) Foster, C. M; Csencsits, R.; Baldo, P. M.; Bai, G. R.; Li, Z.; Rehn, L. E.; Wills, L. A.; Hiskes, R.; Dimos, D.; Sinclair, M. B. *Mater. Res. Soc. Symp. Proc.* **1995**, *361*, 307.
(6) Morimoto, A.; Yamanaka, Y.; Minamikawa T.; Shimizu, T. *Mater. Res. Soc. Symp. Proc.* **1995**, *361*, 551.
(7) De veirman, AEM; Timmers, J.; Hakkens, F. J. G.; Cillessen, J. F. M.; Wolf, R. M. *Phillips J. Res.* **1993**, *47*, 185.
(8) Sun, J. Z.; Krusin-Elbaum, L.; Gupta, A.; Xiao, G.; Parkin, S. S. P. *Appl. Phys. Lett.* **1996**, *69*, 1002.
(9) von Helmolt, R.; Wecker, J.; Samwer, K.; Haupt, L.; Barner, K. *J. Appl. Phys.* **1994**, *76*, 6925.
(10) Satyalakshmi, K. M.; Mallya, R. M.; Ramanathan, K. V.; Wu, X. D.; Brainard, B.; Gautier, D. C.; Vasanthacharya, N. Y.; Hegde, M. S. *Appl. Phys. Lett.* **1993**, *62*, 1233.
(11) Raju, A. R.; Aiyer, H. N.; Rao, C. N. R. *Chem. Mater.* **1995**, *7*, 225.

S0897-4756(96)00467-X CCC: $14.00

films, we employed the acetylacetonates of lanthanum and manganese. The $LaMnO_3$ films were deposited on $SrTiO_3$(100) and $LaAlO_3$(100) substrates at 675 K for 5 h and then postannealed in air at 1075 K for 15 h.

The film compositions were determined by energy-dispersive X-ray analysis (EDAX) using an Oxford EDX system attached to a Leica S-440i scanning electron microscope. The crystal structure of the deposited films was studied with a Seifert X-ray diffractometer (Seifert xrd xdl TT, Cu target) equipped with a thin-film attachment. Conventional $\theta-\theta$ scans were collected using a horizontal Bragg Brenatano goniometer and a high-resolution (169 eV) Si(Li) solid-state detector with 0.5 mm/1 mm slits. The step size and step width used for the studies were 0.02° and 1 step/s, respectively.

X-ray rocking curve measurements were performed to gain the information on the crystalline perfection of these films and to quantitate the planar orientation for these films. Both θ and ω rocking scans were conducted on the preselected film peaks known from the $\theta-\theta$ X-ray diffraction pattern. The film thickness was confirmed by cross-sectional scanning electron microscopy.

High-resolution transmission electron microscopy (HREM) was carried out using a JEOL JEM 3010 microscope operated at 300 kV. The specimens suitable for the cross-sectional TEM studies were prepared using the following technique. Two film/substrate pieces were sandwiched face to face with G-I epoxy and held under a vice at an appropriate pressure. Using an ultrasonic disk cutter, 2.3 mm cylinders were drilled and subsequently mounted in a copper tube (3 mm outer diameter and 2.3 mm inner diameter) with epoxy. After the epoxy was cured, the tube was cut into sections 20−30 μm thick, then mechanically polished and dimpled using a GATON dimpler 665. Finally, the thinned specimens were obtained by Ar^+ ion beam thinning by employing a GATON duomill (600DIF).

Standard four-probe conductivity measurements were carried out down to 15 K by using a Lakeshore closed-cycle cryostat and Lakeshore constant current source. For this purpose, ohmic gold contacts were employed by sputtering gold onto the films through a mask. Ferroelectric hysterisis loop measurements were carried out on the PZT films by using a home-built modified Sawyer−Tower circuit.

3. Results and Discussion

3.1. Metallic $LaNiO_3$ Films. The $LaNiO_3$ (LNO) films deposited on $SrTiO_3$(100) substrates were first subjected to the energy-dispersive X-ray analysis (EDAX). The analysis gave the La:Ni ratio to be 1:1 suggesting the stoichiometry to be exact. In Figure 1a, we show the X-ray diffraction pattern ($\theta-\theta$ scan) of LNO deposited on STO showing only the (100), (200), and (300) reflections of LNO and STO, thereby indicating that the film deposited is highly textured. Four-probe electrical resistivity measurements on the LNO film confirmed its metallic nature with a positive temperature coefficient of resistivity. The room-temperature resistivity was 3.2 mΩ cm. To examine the crystallinity of the film in the growth direction, an X-ray rocking curve study was carried out. The ω scan (Figure 1b) of the LNO-(100) reflection gives a full-width at half-maximum (fwhm) of 0.4°, indicating good crystallinity of the film. Thus, the X-ray rocking curve studies show that the LNO/STO film consists of a single (100) growth plane and that the film is epitaxial. The STO(100) substrate promotes the epitaxial growth of the LNO film due to the closeness in the lattice constants between STO (a = 3.905 Å) and LNO (a = 3.846 Å, pseudocubic), the lattice mismatch being just around 1.66%.

The cross-sectional SEM micrograph of the LNO/STO film shown in Figure 2 clearly reveals the film and the substrate regions. From this micrograph, we see that

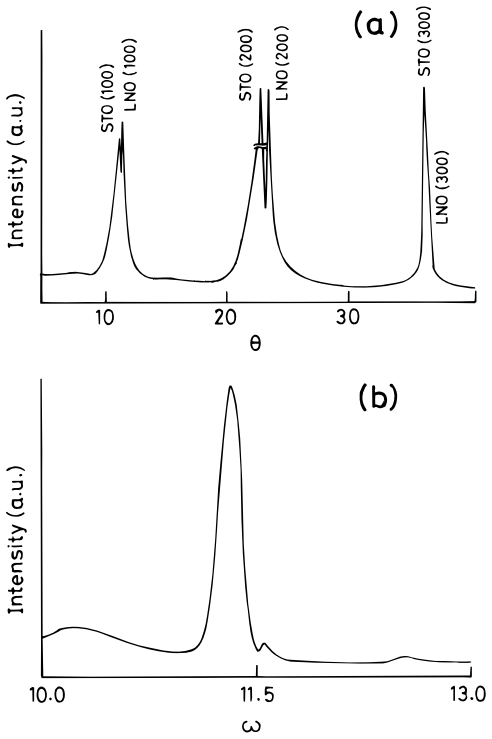

Figure 1. (a) X-ray diffraction pattern ($\theta-\theta$ scan) of a $LaNiO_3$ film deposited on $SrTiO_3$(100) substrate at 675 K for 8 h; (b) rocking curve (ω scan) of the (100) reflection of the film.

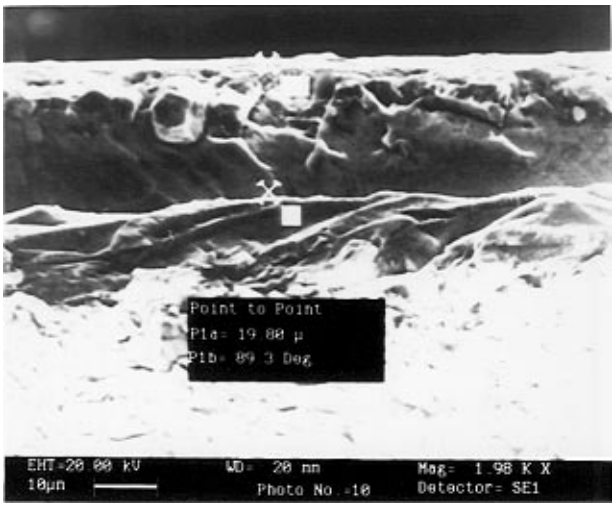

Figure 2. Cross-sectional SEM micrograph of the LNO film deposited on STO(100). Film thickness is 19.8 μm.

the film thickness is around 19.8 μm and that the film is of high density without columnar growth. No cracking or peeling is observed in the film. In Figure 3a, we show a cross-sectional low-magnifiaction TEM image (bright-field image) of the LNO/STO film. The interface is clearly visible and is well marked by the presence of extinction contours arising out of the slight differential thinnning process of the film and the substrate. The film is continuous and devoid of any grain boundaries or defects. A high-resolution cross-sectional image of the LNO/STO interface is shown in Figure 3b. The bright spots on either side of the interface are about 2.7 Å apart, showing good lattice matching. The selected area diffraction pattern (SAED) given in Figure 3c has features of both the LNO film and the STO substrate with intense Bragg spots corresponding to the $\sqrt{2}$ type of the perovskite cell. We observe that the weak spots

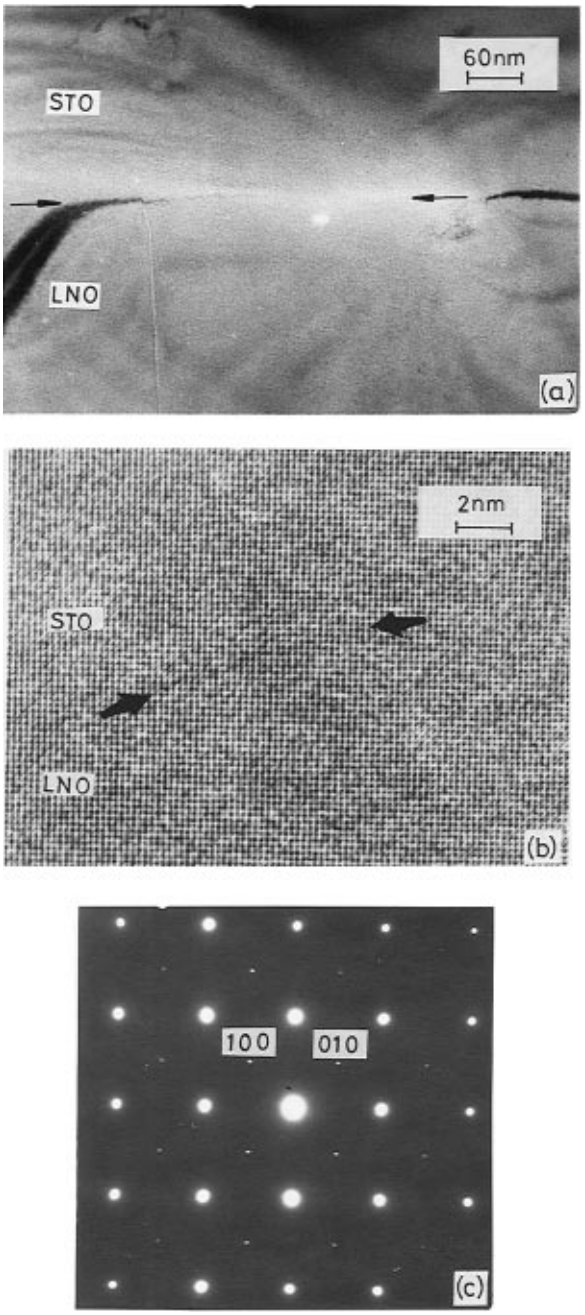

Figure 3. (a) Cross-sectional low-magnification TEM bright-field image of the LNO film deposited on STO(100) showing the interface; (b) HRTEM image of the same interface; (c) SAED pattern from the interface region. (The interface is indicated by the arrows.)

corresponding to 3.9 Å are actually split due to the slight mismatch between the *a* parameters of the LNO film and the underlying STO substrate. The present cross-sectional electron microscopic studies establish the LNO films deposited on STO(100) to be truly epitaxial with the epitaxial relationship of (100)LNO//(100)STO. The quality of the interface of the epitaxial LNO films obtained by us appear to be considerably superior to those obtained by PLD as reported in the literature.[12]

3.2. Ferroelectric $PbZr_{0.5}Ti_{0.5}O_3$ Films. EDAX analysis of the $PbZr_{0.5}Ti_{0.5}O_3$ (PZT) film deposited on a STO(100) substrate gave a Pb:Zr:Ti ratio close to 1:0.5:

(12) Beesabathina, D. P; Salamanca-Riba, L.; Hegde, M. S.; Satyalakshmi, K. M.; Prasad, K. V. R.; Varma, K. B. R. *Mater. Res. Soc. Symp. Proc.* **1994**, *341*, 399.

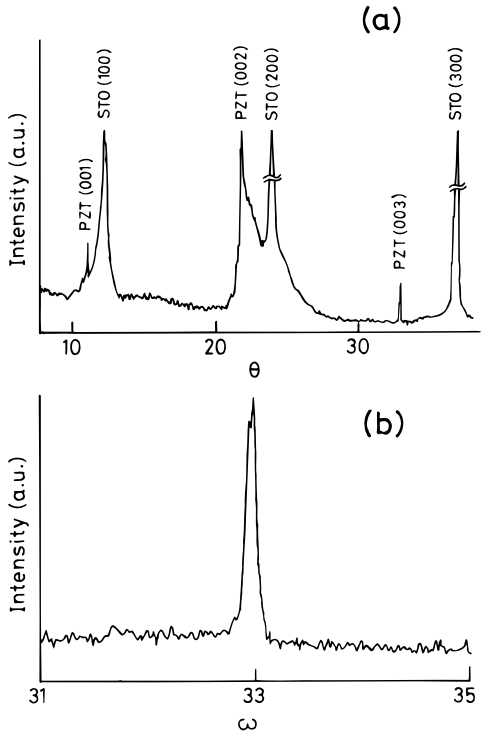

Figure 4. (a) X-ray diffraction pattern ($\theta-\theta$ scan) of a $Pb(Zr_{0.5}Ti_{0.5})O_3$ film deposited on $SrTiO_3$(100) substrate at 625 K for 3 h; (b) rocking curve (ω scan) of the (003) reflection of the film.

0.5. The X-ray diffraction pattern ($\theta-\theta$ scan) of the PZT film (Figure 4a) corresponds to that of the tetragonal phase in the $PbTiO_3-PbZrO_3$ phase diagram. The only reflections observed are those due to $PbZr_{0.5}Ti_{0.5}O_3$. The XRD pattern in Figure 4a indicates that the PZT film on STO(100) is *c*-axis oriented since only the reflections appearing in the pattern are those from the (00*l*) plane (i.e., (001), (002), and (003) reflections) along with the (100), (200), and (300) reflections of the STO substrate. The PZT film deposited by us showed a hysteresis loop characteristic of a ferroelectric with reasonably good values for the coercive field, E_c ($\approx$80 kV cm^{-1}) and remnant polarization, P_r ($\approx$22 C cm^{-2}).

The X-ray rocking curve (ω scan) of the (003) growth plane of PZT is shown in Figure 4b. The rocking curve has a fwhm of 0.2°, indicating an excellent alignment in the growth direction among the *c*-axis-oriented grains. Also, the fwhm value compares well with that of epitaxial ferroelectric films prepared by PLD and MOCVD.[5,6] The epitaxial deposition of PZT film on STO(100) substrate is favored by the reasonably good lattice matching between STO (a = 3.905 Å) and PZT (c = 4.1 Å). The scanning electron micrograph of the PZT film in cross-sectional view (Figure 5) shows the film to be quite smooth, uniform, and densely packed with a thickness of 530 nm.

Cross-sectional transmission electron microscopy of the PZT/STO film revealed the film to be a single domain. No 90° domains were observed in the bright-field images. This may be due to the fact that PZT films in the present experiments were deposited below the Curie temperature. In Figure 6a, we show a high-resolution TEM image of the PZT/STO interface. A direct correspondence between the crystallography of the film and the substrate is evident. The (001) planes of PZT and STO are parallel to the interface and the *a*

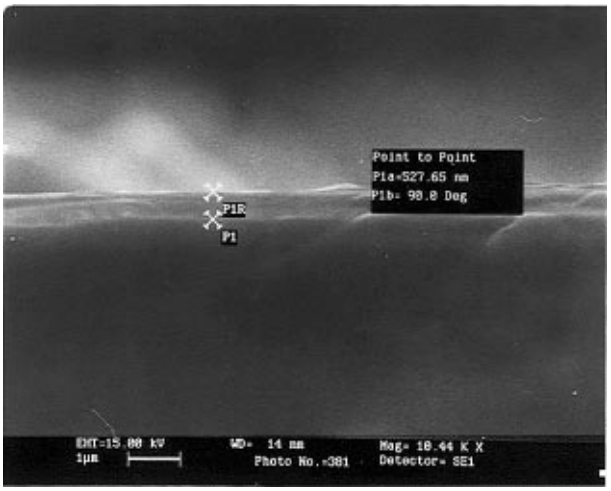

Figure 5. Cross-sectional SEM micrograph of a PZT film deposited on STO(100). Film thickness is 530 nm.

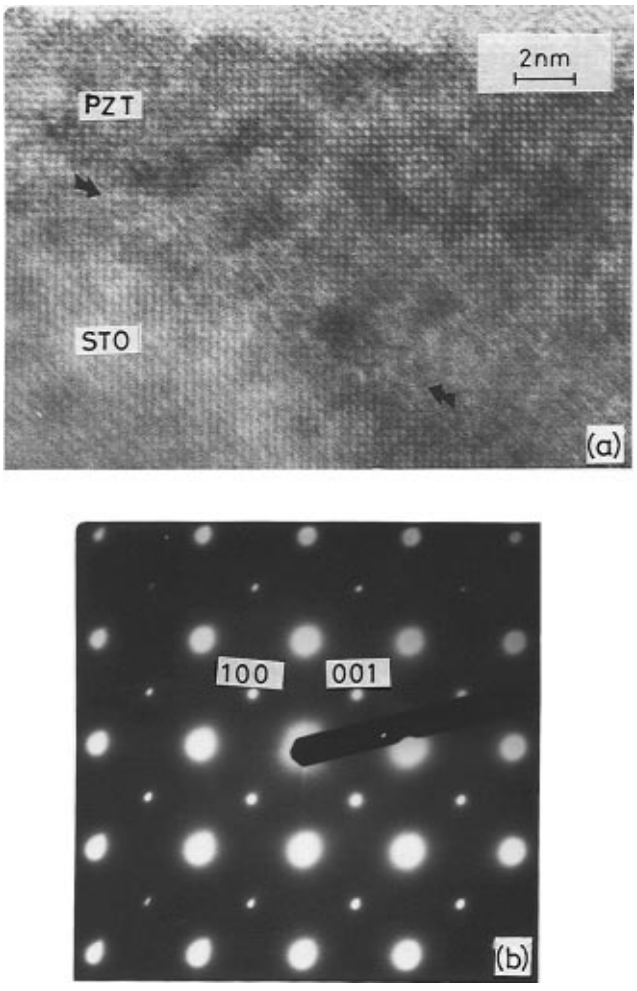

Figure 6. (a) HRTEM image of the PZT/STO interface revealing the epitaxial (*c* oriented) growth of PZT film. The interface is indicated by the arrows. (b) SAED pattern from the PZT/STO interface region.

and *b* axes (i.e., the ⟨100⟩ and ⟨010⟩ directions) of PZT are aligned with the corresponding directions of STO in the interfacial plane, demonstrating the epitaxial nature of the PZT film. The HREM interface image obtained by us is excellent and as good as the literature images of epitaxial ferroelectric films obtained by PLD.[7] The SAED pattern from the PZT/STO interface region shown in Figure 6b gives interplanar spacings (derived from the Bragg spot separations) of 4 Å corresponding to the (100) and (001) reflections. There is little doubt therefore that the epitaxial growth of $PbZr_{0.5}Ti_{0.5}O_3$ is *c*-axis oriented. This along with the coincidence of SAED pattern of the PZT film with that of STO(100) substrate confirms the epitaxial nature of the PZT film, the epitaxial relationship being (001)PZT//(100)STO.

We notice some disparity in the film thicknesses between $LaNiO_3$ film (19.8 μm) and PZT film (0.5 μm). This is accounted for as follows: These films were grown in different experimental conditions, viz., different deposition times (8 h for $LaNiO_3$ and 3 h for PZT), different deposition temperatures (675 K for $LaNiO_3$ and 625 K for PZT). Besides, the $LaNiO_3$ films were deposited using the acetylacetonates of lanthanum and nickel as precursors, whereas PZT films were deposited employing lead acetate and alkoxides of zirconium and titanium as precursors. Acetylacetonates decompose at a lower temperature (~425 K) and alkoxides decompose at a slightly higher temperature. These factors could influence the thickness of the deposited film. It should be noted that we have also obtained epitaxially oriented growth in these systems ($LaNiO_3$ and PZT) deposited at 675 and 625 K, respectively, the film thicknesses being of the order of 0.2 μm. We therefore suggest that the epitaxial growth observed by us in these oxide systems is primarily induced by the lattice matched substrates. The moderate substrate temperature employed by us also promotes the uniform orientation of nucleation resulting in the epitaxial growth.

3.3. $LaMnO_3$ Films Exhibiting Giant Magnetoresistance. The compositions of the $LaMnO_3$ (LMO) films deposited on STO and $LaAlO_3$ (LAO) substrates as determined by EDAX analysis gave the expected La:Mn ratio of 1:1. The X-ray diffraction pattern ($\theta-\theta$ scan) of the LMO film on STO(100) substrate shown in Figure 7a reveals that the film is a single perovskite cubic phase with $a = 3.88$ Å and that it is highly oriented along the (100) direction of STO(100) substrate.

$LaMnO_3$ containing around 30% Mn^{4+} has been shown to possess cubic structure.[13,14] The Mn^{4+} ions arise not because of oxygen excess, but due to the presence of roughly equal number of vacancies on both the La and Mn sites.[15] These A-site vacancies are present randomly and do not give rise to extended defects. Thus, the cubic LMO phase obtained by us can be approximately described as $La_{0.95}Mn_{0.95}O_3$. Electrical resistivity measurements on some of the films deposited by us showed the insulator−metal transition around 200 K, which is close to the ferromagnetic curie temperature.[16]

X-ray rocking curve (ω scan) of the (100) LMO peak shown in Figure 7b is about 0.15° wide indicating a high degree of alignment of the film growth planes with respect to the (100) STO substrate surface, thus indicating the epitaxial nature of the film. In Figure 8a, we show the LMO/STO interface lattice image as obtained by the cross-sectional HREM study. The interfacial

(13) Verelst, M.; Rangavittal, N.; Rao, C.N. R.; Rousset, A. *J. Solid State Chem.* **1993**, *104*, 74.
(14) Mahesh, R.; Kannan, K. R.; Rao, C.N. R. *J. Solid State Chem.* **1995**, *114*, 294.
(15) Hervieu, M.; Mahesh, R., Rangavittal, N.; Rao, C. N. R. *Eur. J. Solid State Inorg. Chem.* **1995**, *32*, 79.
(16) Mahendiran, R.; Tiwari, S. K.; Raychaudhuri, A. K.; Ramakrishnan, T. V.; Mahesh, R.; Rangavittal, N.; Rao, C. N. R. *Phys. Rev.* **1996**, *B53*, 3348.

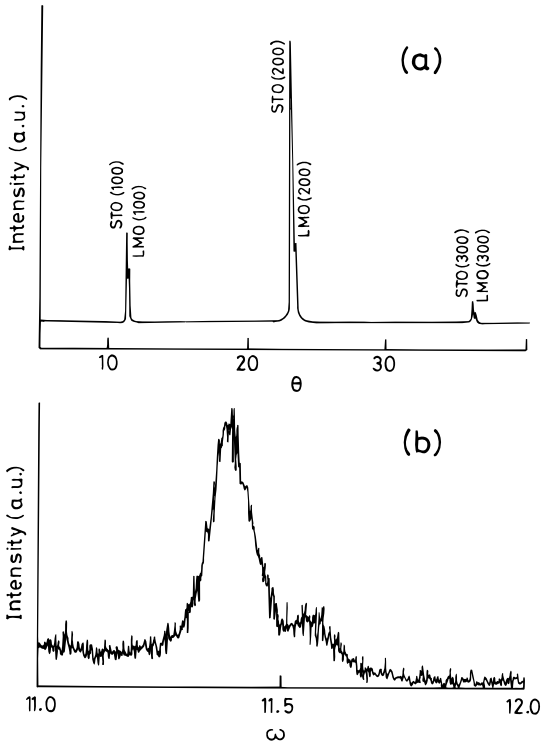

Figure 7. (a) X-ray diffraction pattern ($\theta-\theta$ scan) of a $La_{0.95}Mn_{0.95}O_3$ film deposited on $SrTiO_3$(100) substrate at 675 K for 5 h; (b) rocking curve (ω scan) of the (100) reflection of the film.

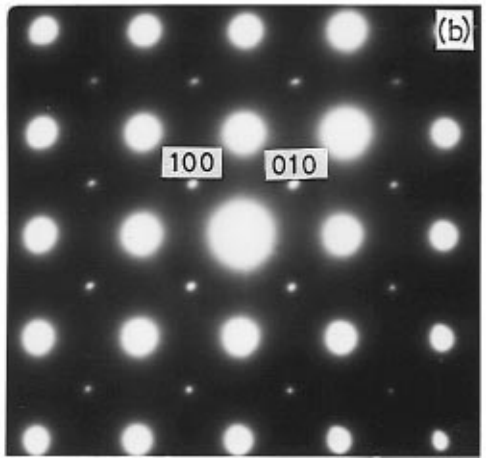

Figure 8. (a) HRTEM image of the LMO/STO interface revealing the epitaxial nature of the film. The interface is indicated by the arrows. (b) SAED pattern from the interface region.

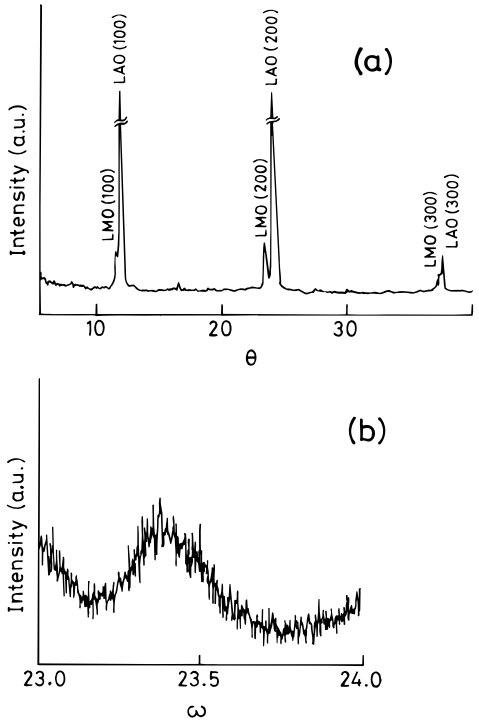

Figure 9. (a) X-ray diffraction pattern ($\theta-\theta$ scan) of a LMO film deposited on $LaAlO_3$(100) substrate at 675 K for 5 h; (b) rocking curve (ω scan) of the (200) reflection of the film.

boundary region does not show any extra phases. The LMO lattice lines are well resolved and extend all the way down to the STO surface closely matching with the STO lattice. The SAED pattern of the LMO/STO interface in Figure 8b shows Bragg spots corresponding to ≈3.9 Å, which split due to the slight mismatch in the *a* parameters. The HREM observations establish the epitaxial growth of the LMO film on STO(100) with the epitaxial relationship of (100)LMO//(100)STO.

We have successfully deposited LMO films on LAO substrate as well. In Figure 9a, the X-ray diffraction pattern ($\theta-\theta$ scan) of the LMO thin film deposited on (100)LAO is shown. The XRD pattern shows a oriented growth as evidenced by the presence of only the (100) and (200) pseudocubic LMO reflections in the $\theta-\theta$ X-ray scan. The rocking curve (ω scan) of the (200)LMO reflection (Figure 9b) shows a fwhm of 0.3°, indicating the epitaxial nature of the film.

We notice that the rocking curves in Figures 7b and 9b exhibit complex structure. This could be possibly due to the nonuniform strain in the sample and also a small misorientation of the grains. Furthermore, the rocking curve for LMO/LAO shown in Figure 9b is broader (fwhm = 0.3°) than the rocking curve for LMO/STO shown in Figure 7b (fwhm = 0.15°) possibly due to the twinned nature of $LaAlO_3$ substrate.

In summary, we have successfully obtained epitaxial films of metallic $LaNiO_3$, ferroelectric $PbZr_{0.5}Ti_{0.5}O_3$, and $LaMnO_3$ showing GMR on single-crystal substrates by means of nebulized spray pyrolysis. We consider this to be an important finding since epitaxial films of such oxide materials are generally obtained by employing rather expensive and more difficult techniques such as MOCVD, PLD, and MBE. It should be noted that we do not find evidence for any polycrystalline component in the X-ray diffraction profiles but observe only oriented peaks even with the high-gain $\theta-\theta$ scan. We therefore

do not find a need to quantify the volume percentage of the epitaxial film. We believe that obtaining good epitaxial films of oxide materials by nebulized spray pyrolysis is a valuable addition to the arsenal of the solid-state and material science.

Acknowledgment. The authors thank the Department of Science and Technology, Government of India, for support. H.N.A. thanks the Council of Scientific and Industrial Research, India for a senior research fellowship.

CM9604672